

EPR and charge-transport studies of polyaniline

V. I. Krinichnyi

Institute of Chemical Physics in Chernogolovka of Russian Academy of Sciences, Chernogolovka, 142432 M.R., Russia

S. D. Chemerisov and Ya. S. Lebedev

N. N. Semenov Institute of Chemical Physics of Russian Academy of Sciences, 117338 Moscow, Russia

(Received 10 December 1996; revised manuscript received 5 February 1997)

The study of dc and microwave (140 GHz) electrical conductivities using multifrequency electron-spin resonance in undoped and HCl-doped polyaniline is reported. The accidental quasi-three-dimensional (3D) charge hopping between the pinned and mobile small polarons dominates the bulk conductivity of the emeraldine base form of polyaniline. The increase in mobility and the number of excitations upon light doping of the polymer leads to the isoenergetic interpolaron charge hopping between the polaron and bipolaron states. 1D variable-range hopping of a charge between conducting islands, which correlates with a superslow torsional dynamics of the polymer chains, dominates bulk conductivity of heavily doped polyaniline at low temperatures. Intrinsic microconductivity is determined by the interaction of the charge with the lattice phonons at high temperatures. Following Epstein and MacDiarmid we propose that emeraldine salt of polyaniline represents a 1D disordered conducting compound consisting of metal-like islands of well coupled chains with 3D delocalized charge carriers. [S0163-1829(97)00524-9]

I. INTRODUCTION

The electronic and magnetic properties of disordered quasi-one-dimensional (1D) semiconductors have been extensively investigated over the past decades.¹⁻⁵ The organic conducting polymers, the electrical conductivity of which can be varied up to the metallic state by doping in the range of more than ten orders of magnitude, is the most interesting class of 1D materials.² In contrast to usual semiconductors, a charge is transferred by the nonlinear topological excitations formed in the chains as a result of Peierls instability,³ namely, solitons in *trans*-polyacetylene (*trans*-PA) and polarons or bipolarons in poly(*p*-phenylene) (PPP) and other PPP-like polymer semiconductors.⁴ The specific nature of such carriers is the reason for unusual charge transport behavior of these organic conducting polymers.

Polyacetylene, the simplest conducting polymer, was studied thoroughly.⁵⁻⁷ To explain the experimental results on the temperature, pressure, and frequency dependencies of electrical conductivity of the lightly doped *trans*-PA, Kivelson proposed a model,⁸ which assumes interchain transport as charge hopping between neutral and charged soliton states at isoenergetic levels. This model was then successfully used by Epstein⁶ for the interpretation of charge transfer in lightly doped *trans*-PA samples. As the doping level increases, isoenergetic charge hopping is replaced by tunneling or hopping between neighboring highly conducting islands⁹ in the framework of the Sheng's¹⁰ and Mott's variable-range hopping¹¹ (VRH) models. The highest room-temperature (RT) conductivity of 10^5 S/cm was achieved for iodine doped and stretch-oriented *trans*-PA.¹² However, this value is by one to two orders of magnitude lower than that predicted by Kivelson and Heeger for a metal-like clusters in the polymer.¹³

The electrical and magnetic properties of doped PPP-like polymers are generally similar to those of *trans*-PA.^{2,14,15} In

contrast with PA, these polymers do not possess a degenerate ground state¹⁶ and, therefore, they are not expected to accommodate single solitons. However, Brédas *et al.*¹⁷ have shown that soliton-antisoliton pairs in the form of polarons and bipolarons could be stabilized in doped PPP. Moreover, Kivelson proposed¹⁸ that the isoenergetic charge transfer might be important not only for *trans*-PA, but also for another conducting polymers possessing solitonlike excitations. Indeed, Kuivalainen *et al.*¹⁹ have shown that the above mechanism plays an important role in both dc and microwave (25 GHz) conductivities of lightly doped PPP. As in the case of *trans*-PA, the VRH was shown experimentally (see, e.g., Refs. 19-22) to be mainly applied also for an interpretation of the conducting properties of different medi-ally and highly doped PPP-like polymers.

In contrast with *trans*-PA and PPP-like conducting polymers, the chains of polyaniline (PANI) contain nitrogen heteroatoms involved in a conjugation.¹⁵ Moreover, benzene rings of PANI can rotate or flip, modulating strong electron-phonon interactions.²³ This results in somewhat of a difference in magnetic and charge-transport properties of PANI compared with other conducting polymers. An analysis of experimental data on the temperature dependencies of dc conductivity, thermoelectric power, and Pauli-like susceptibility allowed MacDiarmid, Epstein *et al.*²⁴ to show that the emeraldine base form of PANI (PANI-EB) is a completely amorphous insulator in which 3D granular metal-like clusters are formed in the course of its transformation into the emeraldine salt form of the polymer (PANI-ES). A more detailed study of the complex microwave dielectric constant, EPR linewidth, and electric field dependence of conductivity of PANI-ES Refs. 20, 22, and 25 allowed them to conclude that both chaotic and oriented PANI-ES consist of some parallel chains strongly coupled into "metallic bundles" between which 1D VRH charge transfer occurs and in which 3D electron delocalization takes place. The intrinsic conductivity of

C. Electron paramagnetic resonance

EPR measurements were performed using *D*-band (140 GHz) EPR5-01 (Ref. 34) and *X*-band (9.8 GHz) PS-100X EPR spectrometers with a 100 kHz magnetic field modulation for a phase-lock detection. Total spin concentration in the samples was determined using an evacuated 10^{-3} M toluene solution of 2,2,6,6-tetramethylpiperidinyloxy radical as a standard by double integration of their *X*-band EPR spectra. Mn^{2+} impurity in MgO powder with $g_{\text{eff}}=2.00102$ and $a=87.4$ G magnetic constants was used at the *D* band as a lateral standard for the determination of the g factor and the calibration of a magnetic field sweep scale. *D*-band EPR spectra were recorded for both imaginary and real terms of the total paramagnetic susceptibility χ in the 90–330 K temperature range. The error of the determination of peak-to-peak linewidth, ΔB_{pp} and g -factor values was $\pm 2 \times 10^{-2}$ G and $\pm 2 \times 10^{-4}$ at the *X* band, and $\pm 5 \times 10^{-2}$ G and $\pm 3 \times 10^{-5}$ at the *D*-band EPR, respectively. The relaxation parameters of the paramagnetic centers in the PANI samples were measured using the steady-state saturation method described in detail earlier.^{7,30}

Paramagnetic centers (PC's) in PANI at the *X*-band demonstrate a Lorentzian single symmetrical spectra the ΔB_{pp} value of which depends on both the doping level and temperature [Fig. 3(a)]. The linewidth of PC in undoped and lightly doped PANI is practically temperature independent at this wave band [Fig. 3(a)], whereas this value of IV-VI PANI samples demonstrates bell-type temperature dependence with some critical temperature $T_c \approx 200$ K. Such an extremality becomes more evident at the growth of y , especially for the heavily doped PANI-ES. The ΔB_{pp} value was observed to increase approximately linearly with temperature at $T \geq T_c$ and to decrease at lower temperatures.

In addition to the unresolved averaged hyperfine structure, the EPR spectrum of PANI indicates also a hyperfine interaction of a small part of the spins with both hydrogen and nitrogen nuclei. As an example, the central regions of the second derivatives of the *X*-band absorption signals of IV and VI PANI-ES samples are presented on Fig. 4. In the first sample an unpaired electron interacts with four nearly equivalent neighboring hydrogen atoms of the lateral benzoid circles possessing nuclear spin $I=1/2$ and with the central nitrogen nucleus with $I=1$ resulting for the appearance of the equidistant well resolved lines with the relative intensities of 1:5:11:14:11:5:1 [Fig. 4(b)]. In addition to these nuclei, an unpaired electron in sample VI interacts also with the fifth nonequivalent hydrogen nucleus located at N atom. This leads to the appearance of an additional splitting in the spectrum [Fig. 4(a)]. The measured constants of hyperfine interaction of an unpaired electron with H and N atoms and calculated spin densities on their nuclei are summarized in Table I.

The typical *D*-band absorption and dispersion EPR spectra of PC in PANI-EB and PANI-ES samples are shown in Fig. 5. At this waveband the PANI EPR spectra became Gaussian with a higher linewidth compared with the *X*-band spectra as it occurs in the case of other conducting polymers.^{7,30} In the dispersion spectra of undoped and lightly doped PANI the bell-like components are registered. The appearance of such a components is attributed to the effect of

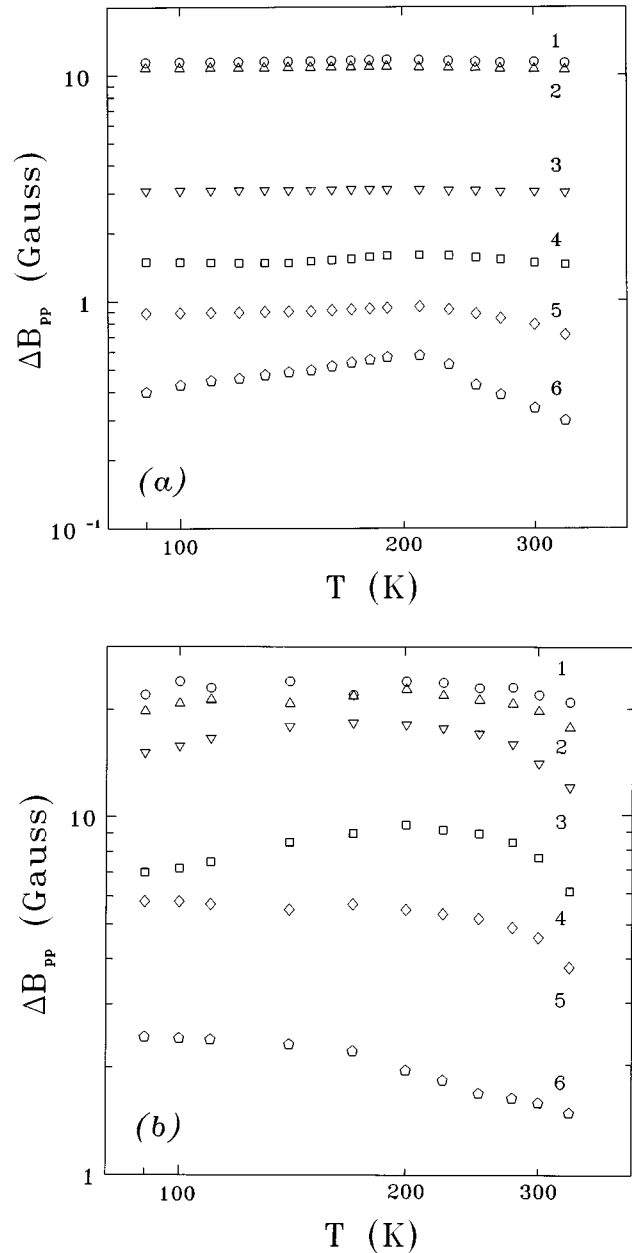


FIG. 3. The plots of the peak-to-peak linewidth of the *X*-band (a) and *D*-band (b) EPR in-phase absorption spectrum of paramagnetic centers in I (1), II (2), III (3), IV (4), V (5), and VI (6) PANI samples versus temperature.

adiabatically fast passage of the separated and saturated spin packets by a modulating magnetic field discussed below.

The plots of ΔB_{pp} versus temperature and doping level for PANI samples are shown in Fig. 3(b). As in the case of *X* band, ΔB_{pp} depends on both temperature and conductivity of the sample, however, with a higher susceptibility to both parameters.

III. DISCUSSION

A. Electron paramagnetic resonance results

The computer simulation showed that *D*-band EPR spectra of the undoped and lightly doped polymers presented in Fig. 5(a) consist of two spectra attributed to PC R_1 and R_2

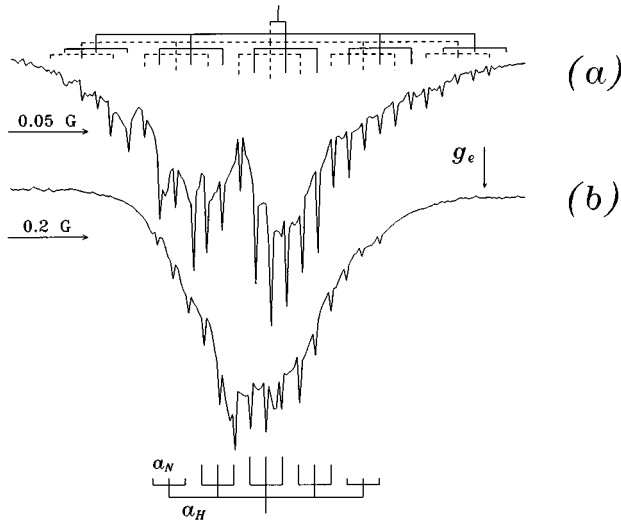


FIG. 4. The center section of the X-band in-phase second harmonic absorption spectra of VI (a) and V (b) HCl-doped PANI powders registered at room temperature. The hyperfine structures, constants of the hyperfine interaction of an unpaired electron with H (a_H) and N (a_N) nucleus, and the position of g factor of free electron ($g_e=2.002\ 32$) are shown.

likely stabilized in PANI-EB and PANI-ES traces in the former, respectively. Radical R_1 demonstrates the strongly anisotropic spectrum with the canonic components $g_{xx}=2.005\ 22$, $g_{yy}=2.004\ 01$, and $g_{zz}=2.002\ 28$ of g tensor, and hyperfine coupling constant $A_{zz}=22.7$ G. Radicals R_2 are registered at $g_{\perp}=2.004\ 63$ and $g_{\parallel}=2.002\ 23$. Assuming $A_{xx}=A_{yy}=12.5$ G for PC in the pernigraniline base³⁵ and the McConnell proportionality constant for the hyperfine interaction of the spin with a nitrogen nucleus $Q_N=23.7$ G (Ref. 36) the spin density on N nucleus $\rho_N^{\pi}(0)=(A_{xx}+A_{yy}+A_{zz})/(3Q_N)=0.62$ can be estimated. Using the above mentioned values of the g -tensor components, $g_e=2.002\ 32$ for a free electron and λ_N equal for ^{14}N to 9.4 meV (Ref. 37) the energies of the lowest induced electron excitative transitions have been calculated from the relation³⁶

$$g_{xx,yy}-g_e=\frac{g_e\rho_N^{\pi}\lambda_N}{\Delta E_{ij}} \quad (1)$$

TABLE I. The hyperfine interaction constant a_i (in Gauss) and spin densities on H and N nuclear ρ_i (in 10^{-3}) of the PANI samples. Note that the ρ values were calculated using the McConnell relation $a=Q\rho(0)$ and Q proportionality constant equal to 22.5 and 23.7 G (Refs. 36 and 37 for H and N atoms, respectively). The values calculated for the central H atom are marked by the * symbol.

Value	Samples					
	I	II	III	IV	V	VI
a_H	4.1	3.1	2.8	0.24	0.14	0.053
a_H^*						0.0095
a_N	1.4	1.0	0.92	0.076	0.046	0.018
ρ_H	182	138	124	107	6.22	2.36
ρ_H^*						0.422
ρ_N	59.1	42.2	38.8	3.21	1.94	0.760

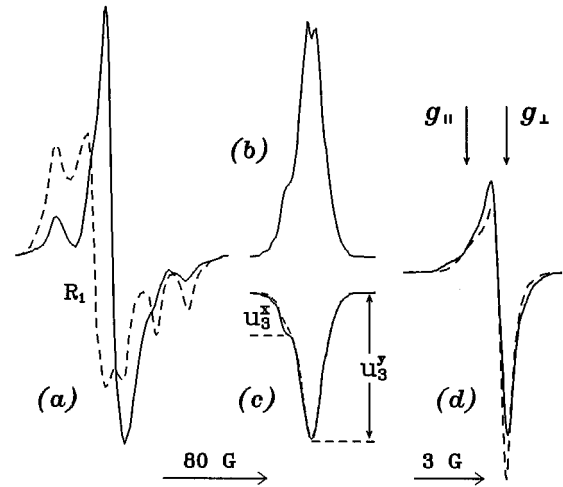


FIG. 5. D-band in-phase absorption (a,d), in-phase dispersion (b), and $\pi/2$ -out-of-phase dispersion (c) spectra of I (a-c) and VI (d) PANI samples registered at room temperature in an inert atmosphere. The simulated spectrum of the paramagnetic centers R_1 (a) and the spectra registered at 200 K (c,d) are shown by dotted lines. The components u_3^x and u_3^y of the $\pi/2$ -out-of-phase dispersion spectrum (c) and the components g_{\parallel} and g_{\perp} of the paramagnetic centers R_2 (d) are shown as well.

to be $\Delta E_1=3.77$ eV and $\Delta E_2=6.17$ eV. The RT relative concentration ratio of PC R_1 , $n_1/(n_1+n_2)$ is equal approximately to 0.3 and decreases with the temperature and doping level increase. Radical R_2 in the sample VI demonstrates the axial-symmetric spectrum with $g_{\perp}=2.003\ 38$ and $g_{\parallel}=2.003\ 61$ [Fig. 5(d)]. It is necessary to note that the replacement of $g_{\perp}>g_{\parallel}$ inequality by an opposite one at the PANI doping increase from $y=0$ up to $y\geq 0.2$ evidences for the restructuring of the polymer lattice associated with the percolation process. As the averaged g factor, $\langle g \rangle_1 = \frac{1}{3}(g_{xx}+g_{yy}+g_{zz})$ of R_1 is approximately equal to that of radical R_2 , $\langle g \rangle_2 = \frac{1}{2}(2g_{\perp}+g_{\parallel})$, one can conclude that radical R_1 is polaron pinned on the polymer chain, whereas R_2 is the same nonlinear excitation moving along the chain with the minimum rate³⁸

$$\nu_{1D}^0 \geq \frac{(g_{xx}-g_e)\mu_B B_0}{h}, \quad (2)$$

where μ_B is the Bohr magneton, B_0 is the strength of the external magnetic field, and h is the Planck constant. So then $\nu_{1D}^0 \geq 5.5 \times 10^7 \text{ sec}^{-1}$ was obtained for the heavily doped PANI-ES sample. The linewidth of the perpendicular component of RT both X- and D band spectra for radical R_2 changes with y . This fact can be associated not only with the increase in the charge carriers mobility but also with the decrease of a spin density on the nitrogen atom and with the change of the polymer chains conformation. The transfer integral I_{C-N} between nitrogen p_z and carbon p_z orbitals at the *para*-position of benzene rings of PANI has an $I_{C-N} \propto \cos\theta$ dependency from ring-N-ring dihedral angle θ , typical for other hydrocarbons.³⁹ Taking $\theta=56^\circ$ for PANI-EB,⁴⁰ the effective θ and $\rho_N^{\pi}(0)$ values were calculated from Eq. (1) to be 33° and 0.42, respectively. Such an angle θ decrease leads to the increase in the spin density on benzene rings due to the

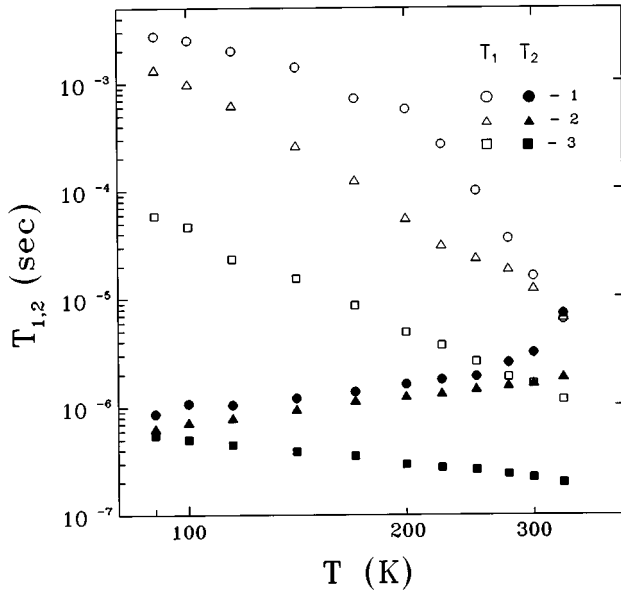


FIG. 6. Temperature dependence of the effective spin-lattice T_1 (open points) and spin-spin T_2 (shaded points) relaxation times of the paramagnetic centers in the initial I (1) and in the II (2) and III (3) HCl-doped PANI samples.

increase of I_{C-N} integral. Therefore, the above mentioned change in magnetic parameters can signify the higher spin delocalization along the polymer chains and a higher conductivity of PANI-ES due to a more planar conformation of its chains.

The increase in the operating magnetic field strength should lead to the drastic decrease of exchange interaction between neighboring paramagnetic centers.⁴¹ Therefore, the transition from the X-band to D-band should lead to the saturation of individual spin packets^{42,43} at sufficiently low radiofrequency power. This effect was observed in our case [Figs. 5(b,c)] and does not register earlier in a study of different conducting polymers at lower magnetic fields. In general, the equation for the first derivative of dispersion signal U can be written as⁴³

$$U' = u_1(\omega_m t) + u_2 \sin(\omega_m t - \pi) + u_3 \sin(\omega_m t - \pi/2), \quad (3)$$

where ω_m is the angular frequency of modulation magnetic field. $\omega_m T_1 > 1$ inequality is realized for the initial and low-doped PANI samples, therefore their dispersion spectra registered at an adiabatic fast passage of the saturated spin packets are determined mainly by the two last terms of Eq. (3) [Figs. 5(b) and 5(c), respectively]. Figure 6 presents the temperature dependencies of the effective spin-lattice T_1 and spin-spin T_2 relaxation times of these samples determined separately from the analysis of u_2 and u_3 components' intensities of their dispersion spectra according to the method described earlier.^{7,30} These dependencies show that the relaxation times are drawn together as the sample doping level increase indicating the intensification of an interchain coupling during this process.

Both the intensity and the shape of the dispersion signal U depend not only on a spin exchange and on an electron relaxation but also on a comparatively slow macromolecular reorientation in the samples. In the framework of the satura-

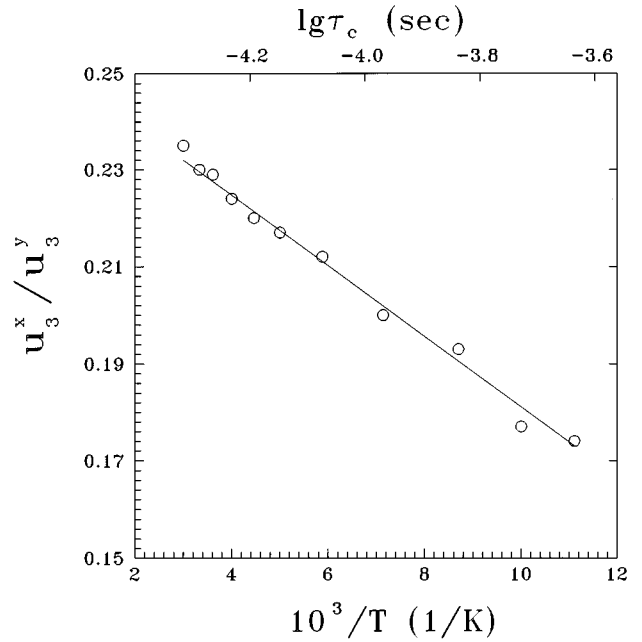


FIG. 7. Temperature dependence of the ratio u_3^x/u_3^y given from the $\pi/2$ -out-of-phase dispersion spectrum presented in Fig. 5(c) (points). The logarithmic dependence of this ratio on the correlation time $\tau_c^x = 5.4 \times 10^{-8} (u_3^x/u_3^y)^{-4.8}$ sec of X-anisotropic polymer chain librations is shown by a solid line.

tion transfer (ST-EPR) method⁴⁴ the correlation time of the latter process, τ_c varies from approximately 10^{-7} sec up to a maximum value

$$\tau_c^{\max} = \frac{2}{3 \pi^2 T_1 \gamma_e^2 B_1^4} \frac{\sin^2 \Theta \cos^2 \Theta (B_{\perp}^2 - B_{\parallel}^2)^2}{B_{\perp}^2 \sin^2 \Theta + B_{\parallel}^2 \cos^2 \Theta}, \quad (4)$$

where γ_e is the gyromagnetic ratio for electron, B_1 is the amplitude of magnetic component of a polarizing radiofrequency field, Θ is the angle between the directions of an external magnetic field B_0 and a molecular x axis of a radical, and B_{\perp} and B_{\parallel} are the low- and high-field spectral component arrangements along the scanning field, respectively.

Earlier we have shown³⁰ that the correlation time of the spin and therefore the chain reorientations near the polymer x axis can be calculated in the framework of the ST-EPR method analyzing the shape of $\pi/2$ -out-of-phase dispersion signal, i.e., the u_3^x/u_3^y ratio [Fig. 5(c)] from the equation

$$\tau_c^x = \tau_0 \left(\frac{u_3^x}{u_3^y} \right)^{-m}. \quad (5)$$

Figure 7 presents the Arrhenius dependence of the correlation time $\tau_c^x = 3.5 \times 10^{-5} \exp(0.015 \text{ eV}/(k_B T))$, sec of macromolecular librations in the initial PANI samples, determined from its ST-EPR spectra by using Eq. (5) with $\tau_0 = 5.4 \times 10^{-8}$ sec and $m = 4.8$. Similar dependencies were also obtained for II and III samples. τ_c^{\max} , calculated using Eq. (4) with $\Theta = 45^\circ$, $B_1 = 0.1 \text{ G}$,³⁴ g_{xx} and g_{zz} values measured for R_1 center, is equal to 1.3×10^{-4} sec and corresponds to $u_3^x/u_3^y = 0.22$ [see Eq. (5)] at 125 K.

In order to interpret electron spin relaxation in I-III PANI samples we assumed that polarons diffuse along the polymer

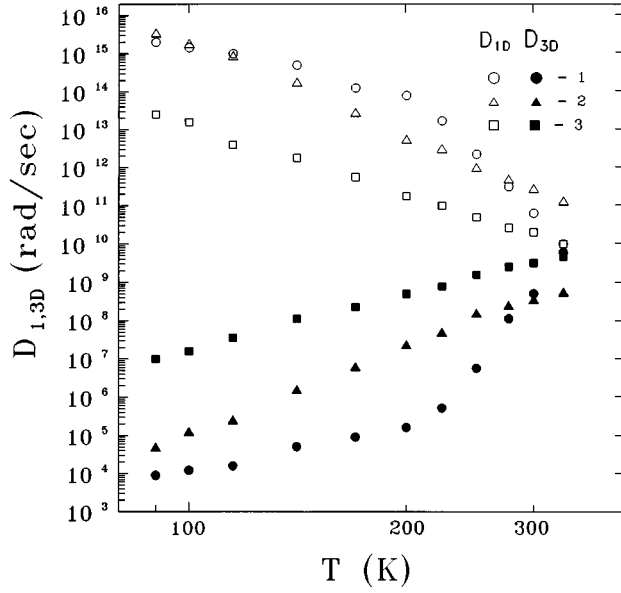


FIG. 8. Temperature dependence of in-chain diffusion D_{1D} (open points) and interchain hopping D_{3D} (shaded points) rates of mobile paramagnetic centers in the initial I (1) and in the II (2), III (3) HCl-doped powder PANI samples determined using Eqs. (6)–(8).

chains and hop between them, respectively, with the rate constants of D'_{1D} and D_{3D} . The spectral density function of this motion is³⁰

$$J(\omega_e) = n\phi(\omega_e) \sum_{ij}, \quad (6)$$

where $n = n_1 + n_2/\sqrt{2}$ is the total concentration of the radicals R_1 and R_2 with, respectively, n_1 and n_2 spin concentrations per one monomer unit, the Fourier fluctuation power spectrum for 1D spin motion $\phi(\omega_e)$ is equal to⁴⁵ $(2D'_{1D}\omega_e)^{-1/2}$ at $D_{1D} > \omega_e > D_{3D}$ and to $(2D'_{1D}D_{3D})^{-1/2}$ at $\omega_e \rightarrow 0$, $D'_{1D} = 4D_{1D}N_p^{-2}$, N_p is the length of a spin delocalization on the polaron repeating units, ω_e is the angular frequency of the spin precession, and \sum_{ij} is the powder averaged lattice sum. Note, that the analogous power spectrum was used also by Mizoguchi *et al.*²⁷ in the investigation of spin dynamics in PANI samples. The electron-spin relaxation is determined mainly by a dipole-dipole interaction between radicals of different mobility possessing spin $S=1/2$, therefore, we can write for the spin relaxation rates^{37,46}

$$T_1^{-1} = \langle \omega^2 \rangle [2\phi(\omega_e) + 8\phi(2\omega_e)], \quad (7)$$

$$T_2^{-1} = \langle \omega^2 \rangle [3\phi(0) + 5\phi(\omega_e) + 2\phi(2\omega_e)], \quad (8)$$

where $\langle \omega^2 \rangle = 0.1\gamma_e^4\hbar^2S(S+1)n\sum_{ij}$ is the averaged sum of the spin dipolar interaction for powder.

Figure 8 shows the temperature dependencies of D_{1D} and D_{3D} calculated at averaged⁴⁷ $N_p \approx 5$ from Eqs. (7) and (8) using the data for the samples I–III presented in Fig. 6. These constants were obtained to be $D_{1D} \approx 10^{11}$ rad/sec and $D_{3D} \approx 10^8$ rad/sec at room temperature. The first value is lower by approximately two orders of magnitude than that

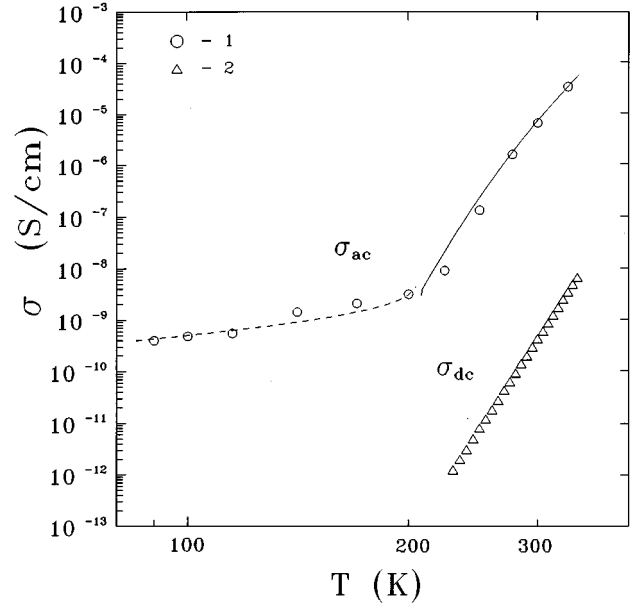


FIG. 9. Temperature dependencies of the ac (1) conductivity of I PANI-EB sample determined using Eq. (9) and data presented in Fig. 8, and dc (2) one. ac conductivities calculated from Eq. (10) with $\sigma_0 = 1.3 \times 10^{-8}$ S/(cm eV), $h\nu_{ph} = 0.017$ eV, and $E_H = 0.073$ eV (dashed line) and Eq. (11) with $\sigma_0 = 14.5$ S eV/cm, $E_H = 0.073$ eV and $E_a = 0.40$ eV (solid line) are shown as well.

earlier reported for $y \leq 0.05$ PANI sample²⁷ but considerably higher than ν_{1D}^0 calculated above.

B. Conductivity and charge transport in undoped PANI

Instead of the dependence $\sigma_{dc}(T) \propto T^{13.5}$ typical for *trans*-PA,⁶ PANI-EB demonstrates some stronger temperature dependence, $\sigma_{dc}(T) \propto T^{22}$ at high temperatures (Fig. 2). The slope of this dependence is approximately the same evaluated from the high-temperature data for PANI-EB reported earlier by Zuo *et al.*⁴⁸ and seems to be too strong to describe the charge transfer in this sample as isoenergetic interpolaron hopping.⁸ Attempts to analyze quantitatively conductivity data of the low-conductive PANI samples in the framework of Mott's VRH conventional model¹¹ for disordered semiconductors always resulted in quite unreasonable values for Mott's parameters, in contrast to the heavily doped case.⁴⁹ So another conduction mechanism should be motivated.

The interchain ac conductivity of the initial PANI-EB sample can be calculated from the data presented in Fig. 8 by using the following well known equation:

$$\sigma_{ac}(T) = \frac{Ne^2D_{3D}b^2}{k_B T}, \quad (9)$$

where N is the volume concentration of the mobile spin excitations and b is the interchain distance in the sample. Figure 9 shows the temperature dependence of σ_{ac} calculated from Eq. (9) with $N = 9.5 \times 10^{17}$ cm⁻³ and $b = 4.39$ Å³¹ compared with the experimental $\sigma_{dc}(T) = 1.4 \times 10^{-64} T^{22}$ one of the sample. These dependencies are quite similar at least at the $T \geq T_c \approx 200$ K temperature region. It is evident that there are two temperature regions divided by the critical tempera-

ture $T_c = h\nu_{\text{ph}}/k_B$ (here ν_{ph} is the $2k_F$ optical phonon frequency) with different slopes of the functions $\sigma_{\text{ac}}(T)$. Such a behavior can be explained by a pure distance dependent charge carriers hopping at temperatures $T \leq T_c$ and by both their energy and distance dependent hopping at $T \geq T_c$ in the framework of the model of ‘‘small polaron’’ tunneling.⁵⁰ For ac conductivity this model yields

$$\sigma_{\text{ac}}(T) = \sigma_0 \left[k_B T + \frac{4E_H}{\ln(2\nu_{\text{ph}}/\nu_e)} \ln \left(1 - \frac{k_B T}{E_H} \ln \frac{2\nu_{\text{ph}}}{\nu_e} \right) \right] \quad (10)$$

at $T \leq T_c$ and

$$\sigma_{\text{ac}}(T) = \frac{\sigma_0}{k_B T} \exp \left(- \frac{E_a + E_H}{k_B T} \right) \quad (11)$$

at $T \geq T_c$, where E_H and E_a are the hopping and activation energies. The temperature dependencies of σ_{ac} calculated using Eq. (10) with $\sigma_0 = 1.3 \times 10^{-8}$ S/(cm eV), $h\nu_{\text{ph}} = 0.017$ eV, $E_H = 0.073$ eV, and Eq. (11) with $\sigma_0 = 14.5$ S eV/cm, $E_H = 0.073$ eV, and $E_a = 0.40$ eV are traced in Fig. 9. The figure evidences for well experimental and theoretical data correlation, therefore one can conclude that the charges are transferred in the sample mainly by mobile small polarons. Note, that a similar $\sigma_{\text{ac}}(T)$ functions were obtained earlier for undoped PANI (Ref. 48) at comparatively low registration frequencies and for lightly doped poly(tetrathiafulvalenes)^{30,50} at different operating frequencies. To confirm the above supposition the electric field dependence of the sample dc conductivity would be additionally analyzed.

C. Conductivity and charge transfer mechanism in lightly doped PANI

In order to explain experimental data on conductivity of lightly doped PANI samples, the model of isoenergetic phonon-assisted charge hopping between soliton bound states proposed by Kivelson for charge transfer in *trans*-PA (Ref. 8) may be used. Later he pointed out¹⁸ that such a process might also be relevant in the other 1D semiconductors in which the charge is transferred by solitonlike excitations or even in *cis*-PA with lightly nondegenerate ground states. In this case the charge hopping would occur between bound soliton-antisoliton pairs such as polaron-bipolaron ones.

It is well known that the behavior of $\sigma_{\text{dc}}(T)$ dependence of PA results from the coupling of solitons to the optical phonons which modulate the system dimerization. Since the quinoid-benzoid transition in organic conducting polymers is also strongly modulated by the optical phonons, the temperature dependence of charge transfer between the polarons in PANI is expected to be similar to that calculated for *trans*-PA,⁸ $\sigma_{\text{dc}}(T) \propto T^n$, where n is a constant equal approximately to 10. As in the case of intersoliton hopping process, the activation energy for interpolaron charge transfer is small enough due to a permanent number of polarons and bipolarons in the system. In contrast to the charge carriers in *trans*-PA, however, both polarons and bipolarons are charged, so then one can write Kivelson’s equations for dc and ac electrical conductivities as¹⁹

$$\sigma_{\text{dc}}(T) = \frac{k_1 e^2 \gamma(T) \xi \langle y_i \rangle}{k_B T R_0} \exp \left(- \frac{2k_2 R_0}{\xi} \right), \quad (12)$$

$$\sigma_{\text{ac}}(T) = \sigma_{\text{dc}}(T) + \frac{e^2 N_i^2 \xi_{\parallel}^3 \xi_{\perp}^2 \langle y \rangle \nu_e}{k_3 k_B T} \left[\ln \frac{2\nu_e}{\gamma(T) \langle y \rangle} \right]^4, \quad (13)$$

where $k_1 = 0.45$, $k_2 = 1.39$, and $k_3 = 384$ are constants, $\gamma(T) = \gamma_0 (T/300 \text{ K})^{n+1}$ is the transition rate of a charge between polaron and bipolaron states, $\langle y \rangle = y_p y_{\text{bp}} (y_p + y_{\text{bp}})^{-2}$, y_p and y_{bp} are the concentrations of polarons and bipolarons, respectively, $\xi = (\xi_{\parallel} \xi_{\perp}^2)^{1/3}$, ξ_{\parallel} , and ξ_{\perp} are, respectively, the average, parallel and perpendicular decay lengths of a polaron or bipolaron wave function, and $R_0 = (4\pi N_i/3)^{-1/3}$ is the typical separation between charged impurities, dopants whose concentration is N_i .

If the conductivity is dominated by interpolaron hopping, $\sigma_{\text{dc}}(T)$ should follow $\sigma_{\text{dc}}(T) \propto T^n$ power law, according to Eq. (12). Such a behavior is really observed for the lightly doped PANI samples (Fig. 2). Therefore, one may state that $\sigma_{\text{dc}}(T)$ obtained for these samples better follows the T^n law predicted by Eq. (12) than Mott’s $T^{-1/2}$ one.

The concentration of mobile spins in II PANI sample is $y_p = 1.2 \times 10^{-4}$ per two benzoid rings. Therefore, taking into account that each bipolaron possesses dual charge, $y_{\text{bp}} = 2.3 \times 10^{-3}$ and $\langle y \rangle = 4.6 \times 10^{-2}$ can be obtained. The concentration of impurity is $N_i = 2.0 \times 10^{19} \text{ cm}^{-3}$, so then $R_0 = 22.8$ Å is obtained for this polymer as well. The prefactor γ_0 in Eq. (12) is evaluated from the $\sigma_{\text{dc}}(T)$ dependence to be $3.5 \times 10^{19} \text{ sec}^{-1}$. Assuming spin delocalization over five polaron sites⁴⁷ along the polymer chain with a lattice constant $c_{\parallel} = 9.50$ Å,²⁵ $\xi_{\parallel} = 11.9$ Å is obtained as well. The decay length of a carrier wave function perpendicular to the chain can be determined from the relation⁸

$$\xi_{\perp} = \frac{b}{\ln(\Delta_0/t_{\perp})} \quad (14)$$

where $2\Delta_0$ is the band gap and t_{\perp} is the hopping matrix element estimated as⁵¹

$$t_{\perp}^2 = \frac{\hbar^4 \omega_{\text{ph}}^3 D_{3D}}{2\pi E_p} \exp \left(\frac{2E_p}{\hbar \omega_{\text{ph}}} \right), \quad (15)$$

where E_p is the polaron formation energy and ν_{ph} is the phonon frequency. Using $2\Delta_0 = 3.8$ eV,⁵² typical for π -conjugated polymers $E_p \approx 0.1$ eV,⁵¹ $D_{3D} = 3.6 \times 10^8$ rad/sec determined from experiment, $\nu_{\text{ph}} = 4.2 \times 10^{12} \text{ sec}^{-1}$ obtained below, $t_{\perp} = 7.1 \times 10^{-3}$ eV, $\xi_{\perp} = 0.79$ Å, and $\xi = 2.0$ Å are obtained for II PANI sample. The similar procedure gives $\langle y \rangle = 7.9 \times 10^{-2}$, $\gamma_0 = 2.1 \times 10^{17} \text{ sec}^{-1}$, $\xi_{\perp} = 0.87$ Å, and $\xi = 2.1$ Å for the III PANI sample with $y_p = 1.1 \times 10^{-3}$ and $y_{\text{bp}} = 1.2 \times 10^{-2}$.

The conductivities of II and III PANI samples were calculated from Eq. (12) to be $\sigma_{\text{dc}}(T) = 2.3 \times 10^{-44} T^{15.2}$ and $\sigma_{\text{dc}}(T) = 1.2 \times 10^{-34} T^{12.1}$, respectively. Figure 10 shows these dependencies in comparison with an experimentally determined functions. $\sigma_{\text{ac}}(T)$ calculated using Eq. (9) with $N = N_i$ and data presented in Fig. 8 and those calculated using Eq. (13) with $n = 15.2$ and $n = 12.1$ respectively, for II and III samples are shown in this figure as well. As it can be seen from Fig. 10(a) there is insufficient coincidence of the

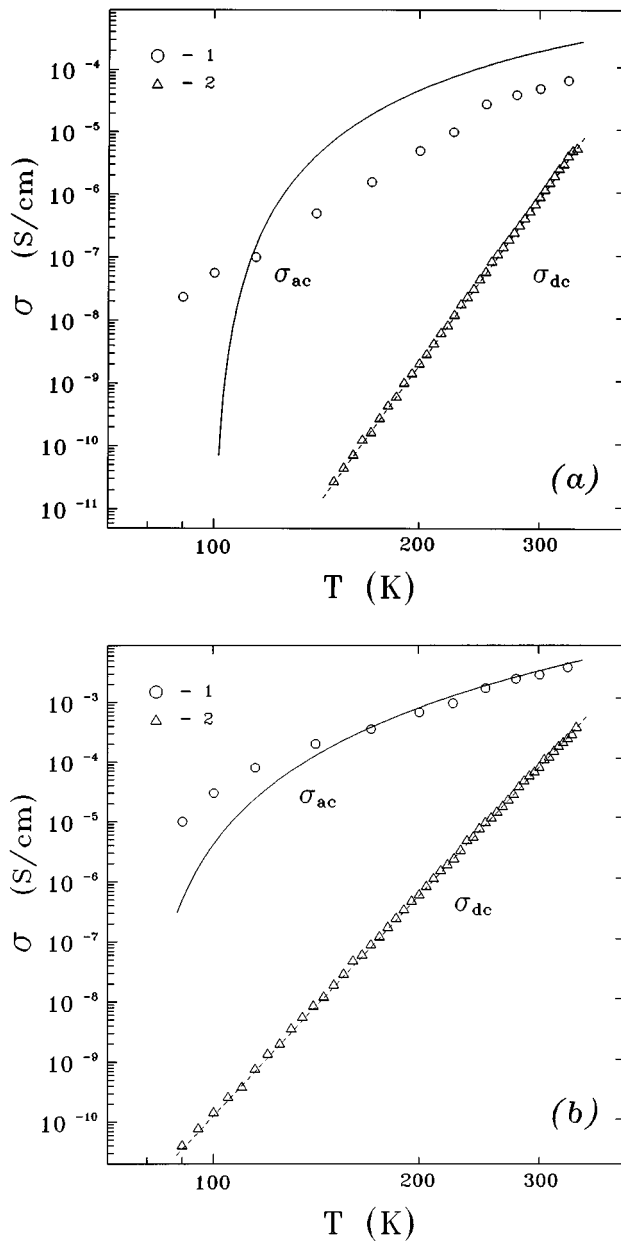


FIG. 10. Temperature dependencies of ac (1) and dc (2) conductivities of II (a) and III (b) HCl-doped powder PANI-ES samples determined using Eq. (9) and the data presented in Fig. 8. The solid lines show ac and dc conductivities calculated using Eqs. (12) and (13) with $n = 15.2$, $\langle y \rangle = 0.046$, $\xi_{\perp} = 0.79$ Å, $\gamma_0 = 3.5 \times 10^{19}$ sec $^{-1}$ (a) $n = 12.1$, $\langle y \rangle = 0.081$, $\xi_{\perp} = 0.87$ Å, $\gamma_0 = 2.1 \times 10^{17}$ sec $^{-1}$ (b), $\xi_{\parallel} = 11.9$ Å, and $\nu_e = 140$ GHz.

theory and experiment in case of II PANI sample. Moreover, the prefactor γ_0 determined for this polymer is higher by approximately two order of magnitude compared with $\gamma_0 = 1.2 \times 10^{17}$ sec $^{-1}$ estimated by Kivelson for *trans*-PA.⁸ The better fitting of an experimental data to the Kivelson's theory is realized in the case of III PANI sample [Fig. 10(b)] for which the value of prefactor γ_0 is approximately the same as that for *trans*-PA. It can be explained by the increase of number and mobility of the mobile charge carriers in higher doped polymer that leads to the increase of a probability of charge hopping between the chains. Therefore, charge transport in an initial polymer is determined by the

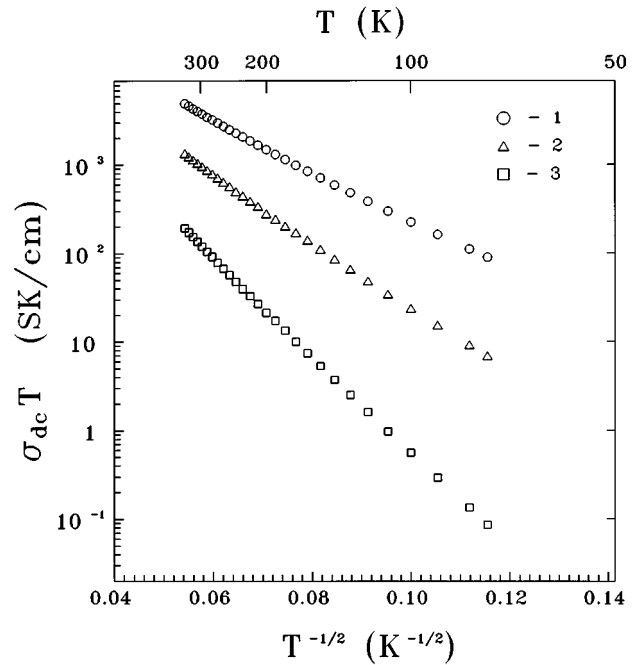


FIG. 11. The dependence of the $\sigma_{dc}T$ product versus $T^{-1/2}$ for VI (1), V (2), and IV (3) HCl-doped PANI-ES samples.

mobility of small polarons. This process is replaced by an isoenergetic charge hopping between the polaron sites at an optimum polymer doping. At lower oxidation of the sample charge transfer is probably realized in the framework of both superposing mechanisms.

D. Conductivity and charge-transport mechanism in heavily doped PANI

Studying dc conductivity and thermoelectric power Wang *et al.*^{20,22} have found that the charge-transport mechanism in PANI-ES samples of different doping levels seems to be 1D variable-range hopping at low temperatures. They have assumed that crystalline fraction of the samples consists of "bundles" of well-coupled chains with 3D extended electron states. Since such domains may be considered as a large-scale clusters of chains, 1D charge transfer between them seems to dominate in the macroscopic conductivity of the polymer. A similar charge transport is probably realized in the heavily doped PANI-ES samples under study.

Figure 11 shows that dc conductivity of IV-VI PANI-ES samples follows well Mott's $T^{-1/2}$ law for 1D VRH charge transport,^{11,53}

$$\sigma_{dc}(T) = k_1 \nu_0 e^2 \frac{n(\epsilon_F) T_0}{\langle L \rangle T} \exp \left[- \left(\frac{T_0}{T} \right)^{1/2} \right], \quad (16)$$

where $k_1 = 1.8$ is a constant, ν_0 is a jump rate prefactor, $n(\epsilon_F)$ is the density of states at the Fermi level ϵ_F , $T_0 = 16/[k_B n(\epsilon_F) \langle L \rangle^3]$ is the percolation constant or effective energy separation between localized states depending on the degree of disorder in amorphous regions, $\langle L \rangle = (L_{\parallel} L_{\perp}^2)^{1/3}$, L_{\parallel} , and L_{\perp} are the averaged length of charge wave function localization and its projections in parallel and perpendicular directions, respectively. T_0 values evaluated from the slopes of the $\sigma_{dc}(T)$ dependencies (Fig.

TABLE II. The percolation constant T_0 (in 10^3 K), spin concentration N (in 10^{19} spin/cm³), the density of states $n(\varepsilon_F)$ at the Fermi level ε_F (in eV⁻¹mole⁻¹), the averaged $\langle L \rangle$, parallel L_{\parallel} , and perpendicular L_{\perp} lengths (in Å) of charge wave function localization in the PANI samples.

Value	Samples					
	I	II	III	IV	V	VI
T_0				10.2	3.76	1.65
N	0.20	0.37	2.1	18	76	153
$n(\varepsilon_F)$				0.6	1.7	3.8
$\langle L \rangle$				20.2	19.1	19.2
L_{\parallel}				71	69	70
L_{\perp}				11	10	10

11) and the averaged localization lengths $\langle L \rangle$ of a charge in the samples determined from $n(\varepsilon_F)$ are presented in Table II. Using the method proposed by Wang *et al.*,²² L_{\parallel} and L_{\perp} components of $\langle L \rangle$ value are obtained as well (Table II). Prefactor ν_0 is calculated using Eq. (16) to vary in $(3.4-4.8) \times 10^{12}$ sec⁻¹ region that is near to $\nu_0 = 1.6 \times 10^{13}$ sec⁻¹ evaluated from the data obtained by Wang *et al.*²⁰ for PANI-ES. So then the phonon frequency can be obtained from the equation $\nu_{\text{ph}} = kT_c/h = 4.2 \times 10^{12}$ sec⁻¹ to fall into the region for ν_0 determined above.

As dipole interaction between the spin packets strongly increases at polymer doping due to formation of the metal-like clusters, therefore an effective relaxation time of PC becomes considerably smaller than ω_m^{-1} , so that the sensitivity of the saturation methods to a spin relaxation and dynamics decreases. In this case the charge mobility in high-conductive PANI-ES can be evaluated from the analysis of the polymer absorption line containing a Dyson⁵⁴ contribution. As one can see from Fig. 5(d), the asymmetry of an absorption line of the heavily doped PANI-ES sample is changed with temperature demonstrating the Dyson behavior. This fact indicates the decrease of a thickness of skin-layer δ on the polymer surface due to the growth of the clusters' intrinsic conductivity as it occurs in some inorganic substances⁵⁵ and organic single crystalline⁵⁶ and polymeric^{30,57,58} conductors.

Figure 12 represents $\sigma_{\text{ac}}(T)$ dependencies of the metal-like clusters in some PANI-ES samples determined according to the method proposed by Wilamowski *et al.*⁵⁵ for amorphous semiconductors of lower dimensionality from the well known equation

$$\delta = \frac{c}{\sqrt{2\pi\omega_e\sigma_{\text{ac}}}}. \quad (17)$$

The figure exhibits a maximum of $\sigma_{\text{ac}} = 1.2 \times 10^4$ S/cm lying near the critical temperature $T_c \approx 200$ K determined above for the samples of lower doping levels. Maximum σ_{ac} is higher by approximately two orders of magnitude than that determined by Joo *et al.*²⁶ at 6.5 GHz for PANI-ES doped by camphor sulfonic acid up to $y = 0.50$. This evidences additionally for 1D electron localization (semiconductive behavior) at $T \leq T_c$ and its 3D delocalization (metallic behavior) in the clusters at higher temperatures. It is important to note

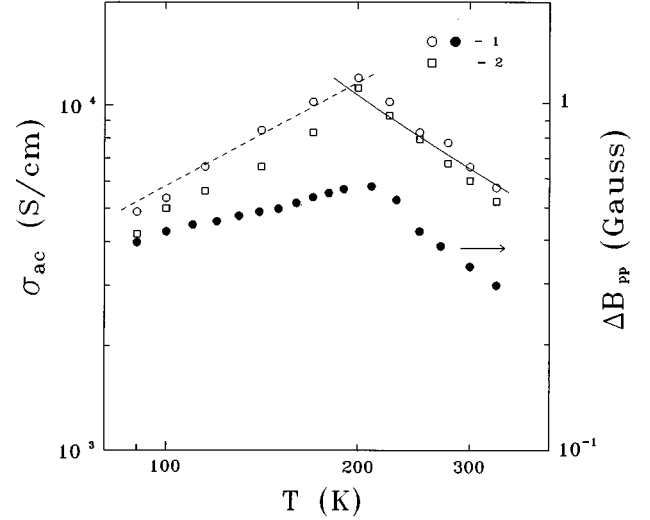


FIG. 12. Temperature dependencies of the intrinsic conductivity σ_{ac} of the VI (1) and V (2) HCl-doped powder PANI samples determined from their EPR line asymmetry and Eq. (17) (points), and those calculated from Eq. (18) with $\langle L \rangle = 16.4$ Å (dashed line), and from Eq. (19) with $c_{\parallel} = 9.50$ Å, and $\alpha = 4.1$ eV/Å. For the comparison the temperature dependence of ΔB_{pp} value for the VI PANI-ES polymer given from Fig. 3(a) is also shown by blacked out points.

that the temperature dependencies of thermoelectric power S , σ_{ac} , and D_{3D} of some conducting polymers reported earlier,^{20,28,59} T_2 , and D_{3D} for PANI-EB and $\Delta B_{pp}(T)$, presented in Figs. 3 and 8, demonstrate a similar temperature behavior at the same temperature region.

Figure 12 shows that at the low temperature region, when $T \leq T_c$, $\sigma_{\text{ac}}(T)$ dependence follows to Mott's VRH law^{11,53}

$$\sigma_{\text{ac}}(T) = \frac{2}{3} \pi^2 e^2 n^2(\varepsilon_F) \langle L \rangle^5 k T \nu_e \left[\ln \frac{\omega_{\text{ph}}}{2\pi\nu_e} \right]^4, \quad (18)$$

whereas at $T \geq T_c$ the conductivity is determined by phonon scattering according to the undimerized SSH model proposed for intrinsic conductivity in *trans*-PA and other conducting polymers,^{13,60}

$$\sigma_{\text{ac}}(T) = \frac{e^2 \omega_{\text{ph}} M I_0^2}{2\pi \hbar^2 c \alpha^2} \sinh \left(\frac{\hbar \omega_{\text{ph}}}{kT} \right), \quad (19)$$

where M is the total mass of CH group, c is the elemental cell constant, and α is the electron-phonon coupling constant. As it is seen from Fig. 12, Eqs. (18) and (19) well approximate the $\sigma_{\text{ac}}(T)$ dependence experimentally obtained for VI PANI-ES at $\langle L \rangle = 16.4$ Å, $c = 9.50$ Å,²⁵ and $\alpha = 4.1$ eV/Å.¹³ Therefore, we can conclude that in PANI-ES charge carriers variable-range hop at low temperatures and are scattered on lattice optical phonons when the phonon energy becomes comparable with $k_B T \geq k_B T_c$.

Aasmundtveit *et al.*⁶¹ have shown that X-band linewidth and consequently the spin-spin relaxation rate of PC in PANI depend directly on its dc conductivity. The comparison of $\sigma_{\text{ac}}(T)$ and $\Delta B_{pp}(T)$ functions presented in Fig. 12 demonstrate the additivity of these values at least at the $T \geq T_c$ region. Besides, Khazanovich⁶² have found that spin-spin re-

laxation depends on the number of spins on each polymer chain N_s and on the number of neighboring chains N_c with which these spins interact as follows:

$$T_2^{-1} = \frac{4\langle\omega^2\rangle}{5\nu_0 N_s} \left[21 \ln \left(\frac{\nu_0}{\nu_e} \right) + 18 \ln N_c \right]. \quad (20)$$

Using $T_2 = 1.7 \times 10^{-7}$ sec, $\sum_{ij} = 1.2 \times 10^{45}$ cm⁻⁶, and $\nu_0 = 4.2 \times 10^{12}$ sec⁻¹ determined from experiment, a simple relation $N_c \approx 55 \exp(N_s)$ of these values is obtained from Eq. (20). This means that at $L_{\parallel} = 70$ Å at least seven interacting spins exist on each chain as a spin packet and interact with $N_c \approx 20$ chains, i.e., spin and charge 3D hopping does not exceed a distance of more than $3b < L_{\perp}$.

The spin motion and the intrinsic conductivity of the sample depend also on the macromolecular dynamics, because the interaction of the spins and charge transfer integral can be modulated by PANI lattice librations as it has happened in other organic crystalline semiconductors.⁶³ One can see from Figs. 7 and 12, that the $\sigma_{ac}(T)$ dependence for the clusters follows $[\tau_c^x(T)]^{-1}$ one for the polymer chain librations at least at $T \leq T_c$.⁶⁴ This means that the lattice librations indeed modulate the interacting spin exchange and consequently the charge transfer integral. Assuming that polaron is covered by both electron and excited phonon clouds, we can propose that both spin relaxation and charge transfer should be accompanied with the phonon dispersion. Such cooperating charge-phonon processes seem to be more important for the doped polymers the high-coupled chains of which constitute 3D metal-like clusters.

The velocity of the charge carriers at the Fermi level, $v_F = 2c_{\parallel} / [\pi \hbar n(\varepsilon_F)]$ is equal to 2.5×10^7 cm/sec for highly doped PANI-ES, so that the rate of the interchain charge hopping can be determined as $D_{3D} = v_F / L_{\perp} = 2.4 \times 10^{14}$ rad/sec, which gives [see Eq. (9)] $\sigma_{ac} = 1.3 \times 10^4$ S/cm at $L_{\perp} = 10$ Å (see Table II) and $T_c \approx 200$ K. The conductivity obtained is close to the ac conductivity evaluated from EPR spectra of the sample (Fig. 12). This fact confirms additionally the existence of metal-like clusters with three dimensionally delocalized electrons in PANI-ES. Therefore, we can calculate the effective mass of charge carries from the relation⁶⁵ $m^* = (3\pi^2 N)^{1/3} \hbar v_F^{-1}$, equal approximately to two free electron masses. The mean free path l_i of the carriers is calculated for this sample⁶⁵ $l_i = \sigma_{ac} m^* v_F / (Ne^2)$ to be as ap-

proximately long as 80 Å at T_c . This value is somewhat smaller than that estimated for oriented *trans*-PA,¹³ but however evidences for extended electron states in this polymer as well.

Thus, the combination of EPR and transport studies confirm the model of 3D electron delocalization in the metal-like clusters and makes it possible to establish the relations between structural and electronic properties of the clusters. In spite of the PANI-EB chain conformation differing from that of other polymers, PANI becomes more planar (see Sec. III A) and conductive during the doping and thus becomes better comparable to other polymers.

IV. CONCLUSION

The data obtained by both high-frequency EPR and electron transport methods show that in undoped PANI the charges are transferred mainly by small polarons, the hopping probability of which strongly depends on the lattice phonon energy. In lightly doped PANI the distribution of site energies is narrowed compared with $k_B T$. This leads to a domination of isoenergetic charge hopping in the polymer, so that both $\sigma_{dc}(T)$ and $\sigma_{ac}(T)$ can be described by the modified Kivelson's model proposed for charge transfer between solitary chains in lightly doped conducting polymers.

As the doping level increases and as the percolation transition takes place the conducting single chains become crystallization centers for the formation of the massive metal-like clusters. This process is accompanied by the increase of the electron-phonon interaction, crystalline order, and interchain coupling. The latter factor plays an important role in the stabilizing of the metallic state, when both 1D electron localization and "Peierls instability" are avoided. Besides, charge transfer is modulated by the macromolecular librations in PANI-ES, the chains of which are strongly coupled and form metal-like clusters with three dimensionally delocalized conducting electrons. This is in agreement with the metal-like "bundles" concept, but contradicts the existence of solitary conducting chains in PANI-ES.

ACKNOWLEDGMENTS

We thank Dr. B. Z. Lubentsov for kindly supplying us with the emeraldine base PANI sample and Dr. A. S. Astakhova for assistance.

¹S. K. Khanna, E. Ehrenfreund, A. F. Garito, and A. J. Heeger, Phys. Rev. B **10**, 2205 (1974); J. F. Kwak, P. M. Chaikin, A. A. Russel, A. F. Garito, and A. J. Heeger, Solid State Commun. **16**, 729 (1975); D. Djerome and H. J. Schulz, Adv. Phys. **31**, 299 (1982); *Highly Conducting Quasi-One-Dimensional Organic Crystals*, edited by E. M. Conwell, Semiconductors and Semimetals, Vol. 27 (Springer-Verlag, Berlin, 1988); A. A. Gogolin, Phys. Rep. **5**, 269 (1988).

²*Handbook of Conducting Polymers*, edited by T. E. Scotheim (Marcel Dekker, Inc., New York, 1986), Vols. 1 and 2; *Electronic Properties of Conjugated Polymers*, edited by H. Kuzmany, M. Mehring, and S. Roth, Springer Series in Solid State Sciences (Springer-Verlag, Berlin, 1987); *Electronic Properties*

of Polymers, edited by H. Kuzmany, M. Mehring, and S. Roth, Springer Series in Solid State Sciences, Vol. 107 (Springer-Verlag, Berlin, 1992); *Polyconjugated Materials*, edited by G. Zerbi (North-Holland, Amsterdam, 1992).

³R. E. Peierls, *Quantum Theory of Solids* (Oxford University Press, London, 1955), p. 108.

⁴A. J. Heeger, in *Handbook of Conducting Polymers*, edited by T. E. Scotheim (Marcel Dekker, Inc., New York, 1986), Vol. 2, p. 729; R. R. Chance, D. S. Boudreaux, J. L. Brédas, and R. Silbey, *ibid.*, p. 825; J. L. Brédas, *ibid.*, p. 859.

⁵J. C. W. Chien, *Polyacetylene: Chemistry, Physics and Material Science* (Academic Press, Orlando, 1984).

⁶A. J. Epstein, in *Handbook of Conducting Polymers*, edited by T.

- E. Scotheim (Marcel Dekker, Inc., New York, 1986), Vol. 2, p. 1041.
- ⁷V. I. Krinichnyi, *Usp. Khim.* **65**, 84 (1996) [Russ. Chem. Rev. **65**, 81 (1996)].
- ⁸S. Kivelson, *Phys. Rev. Lett.* **46**, 1344 (1981); *Phys. Rev. B* **25**, 3798 (1982).
- ⁹H. Stubb, E. Pinkka, and J. Paloheimo, *Mat. Sci. Eng.* **10**, 85 (1993).
- ¹⁰P. Sheng, *Phys. Rev. Lett.* **31**, 44 (1973); *Phys. Rev. B* **21**, 2180 (1980); P. Sheng and J. Klafter, *ibid.* **27**, 2583 (1983).
- ¹¹N. F. Mott and E. A. Davis, *Electronic Processes in Non-Crystalline Materials* (Clarendon Press, Oxford, 1979).
- ¹²H. Naarmann, in *Electronic Properties of Conjugated Polymers* (Ref. 2), p. 12; W. Pukacki, R. Zuzok, and S. Roth, in *Electronic Properties of Polymers* (Ref. 2), p. 12.
- ¹³S. Kivelson and A. J. Heeger, *Synth. Met.* **22**, 371 (1988).
- ¹⁴M. Peo, S. Roth, K. Dransfeld, B. Tieke, J. Hocker, H. Gross, A. Grupp, and H. Sixl, *Solid State Commun.* **35**, 119 (1980); L. W. Shacklette, R. R. Chance, D. M. Ivory, G. G. Miller, and R. H. Baughman, *Synth. Met.* **1**, 307 (1980).
- ¹⁵A. A. Syed and M. K. Dinesan, *Talanta* **38**, 815 (1991).
- ¹⁶W. P. Su, J. R. Schrieffer, and A. J. Heeger, *Phys. Rev. Lett.* **42**, 1698 (1979); *Phys. Rev. B* **22**, 2099 (1980).
- ¹⁷J. L. Brédas, R. R. Chance, and R. Silbey, *Mol. Cryst. Liq. Cryst.* **77**, 319 (1981); *Phys. Rev. B* **26**, 5843 (1982).
- ¹⁸S. Kivelson, *Mol. Cryst. Liq. Cryst.* **77**, 65 (1981).
- ¹⁹P. Kuivalainen, H. Stubb, H. Isotalo, P. Yli-Lahti, and C. Holmström, *Phys. Rev. B* **31**, 7900 (1985).
- ²⁰Z. H. Wang, C. Li, E. M. Scherr, A. G. MacDiarmid, and A. J. Epstein, *Phys. Rev. Lett.* **66**, 1745 (1991); *Phys. Rev. B* **45**, 4190 (1992).
- ²¹M. Rotti, H. Krikor, and P. Nagels, in *Electronic Properties of Conjugated Polymers* (Ref. 2), p. 27; E. Punna, J. Laakso, H. Stubb, and P. Kuivalainen, *Phys. Rev. B* **41**, 5914 (1990); K. Sato, M. Yamaura, T. Hagiwara, K. Murata, and M. Tokumoto, *Synth. Met.* **40**, 35 (1991).
- ²²Z. H. Wang, H. H. S. Javadi, A. Ray, A. G. MacDiarmid, and A. J. Epstein, *Phys. Rev. B* **42**, 5411 (1990); Z. H. Wang, A. Ray, A. G. MacDiarmid, and A. J. Epstein, *ibid.* **43**, 4373 (1991).
- ²³R. P. McCall, J. M. Ginder, M. G. Roe, G. E. Asturias, E. M. Scherr, A. G. MacDiarmid, and A. J. Epstein, *Phys. Rev. B* **39**, 10 174 (1989).
- ²⁴F. Zuo, M. Angelopoulos, A. G. MacDiarmid, and A. J. Epstein, *Phys. Rev. B* **36**, 3475 (1987); A. G. MacDiarmid and A. J. Epstein, *Faraday Discuss. Chem. Soc.* **88**, 317 (1989).
- ²⁵M. E. Jozefowicz, R. Laversanne, H. H. S. Javadi, A. J. Epstein, J. P. Pouget, X. Tang, and A. G. MacDiarmid, *Phys. Rev. B* **39**, 12 958 (1989); J. P. Pouget, M. E. Jozefowicz, A. J. Epstein, X. Tang, and A. G. MacDiarmid, *Macromolecules* **24**, 779 (1991).
- ²⁶J. Joo, E. J. Oh, G. Min, A. G. MacDiarmid, and A. J. Epstein, *Synth. Met.* **69**, 251 (1995).
- ²⁷K. Mizoguchi, M. Nechtschein, J. -P. Travers, and C. Menardo, *Phys. Rev. Lett.* **63**, 66 (1989); K. Mizoguchi, M. Nechtschein, and J. -P. Travers, *Synth. Met.* **41**, 113 (1991).
- ²⁸K. Mizoguchi and K. Kume, *Synth. Met.* **69**, 241 (1995).
- ²⁹D. S. Galvao, D. A. don Santos, B. Laks, C. P. de Melo, and M. J. Caldas, *Phys. Rev. Lett.* **63**, 786 (1989); L. W. Shacklette and R. H. Baughman, *Mol. Cryst. Liq. Cryst.* **189**, 193 (1990).
- ³⁰V. I. Krinichnyi, *2-mm Wave Band EPR Spectroscopy of Condensed Systems* (CRC Press, Boca Raton, 1995); *Usp. Khim.* **65**, 564 (1996) [Russ. Chem. Rev. **65**, 521 (1996)].
- ³¹B. Z. Lubentsov, O. N. Timofeeva, S. V. Saratovskikh, V. I. Krinichnyi, A. E. Pelekh, V. I. Dmitrenko, and M. L. Khidekel, *Synth. Met.* **47**, 187 (1992); F. Lux, G. Hinrichsen, C. Christen, V. I. Krinichnyi, I. B. Nazarova, S. D. Chemerisov, and M.-M. Pohl, *ibid.* **53**, 347 (1993); V. I. Krinichnyi, I. B. Nazarova, S. D. Chemerisov, H. -K. Roth, K. Lüders, F. Lux, and G. Hinrichsen, *Acta Pol.* (to be published).
- ³²V. I. Krinichnyi, S. D. Chemerisov, and Ya. S. Lebedev, *Synth. Met.* **84**, 819 (1997).
- ³³O. Timofeeva, B. Lubentsov, Ye. Sudakova, D. Chernyshov, and M. Khidekel, *Synth. Met.* **40**, 111 (1991).
- ³⁴A. A. Galkin, O. Ya. Grinberg, A. A. Dubinski, N. N. Kabdin, V. N. Krimov, V. I. Kurochkin, Ya. S. Lebedev, L. G. Oranski, and V. Shuvalov, *Prib. Tekh. Éksp.* **4**, 284 (1977); V. I. Krinichnyi, *Appl. Magn. Reson.* **2**, 29 (1991).
- ³⁵S. M. Long, K. R. Cromack, A. J. Epstein, Y. Sun, and A. G. MacDiarmid, *Synth. Met.* **55**, 648 (1993).
- ³⁶A. L. Buchachenko and A. M. Vasserman, *Stable Radicals* (Khimija, Moscow, 1973).
- ³⁷A. Carrington and A. D. McLachlan, *Introduction to Magnetic Resonance with Application to Chemistry and Chemical Physics* (Harper & Row, New York, 1967).
- ³⁸Ch. P. Pool, *Electron Spin Resonance: A Comprehensive Treatise on Experimental Techniques* (Wiley, New York, 1983).
- ³⁹V. F. Traven, *Electronic Structure and Properties of Organic Molecules* (Khimija, Moscow, 1989).
- ⁴⁰J. G. Masters, J. M. Ginder, A. G. MacDiarmid, and A. J. Epstein, *J. Chem. Phys.*, **96**, 4768 (1992).
- ⁴¹S. A. Al'tshuler and B. M. Kozyrev, *Electron Paramagnetic Resonance* (Academic, New York, 1964); *Electron Paramagnetic Resonance of Compounds of Elements of Intermediate Groups* (Nauka, Moscow, 1972).
- ⁴²M. Weger, *Bell. Syst. Tech. J.* **39**, 1013 (1960); A. A. Bugai, *Fiz. Tverd. Tela (Leningrad)* **4**, 3027 (1962); Ya. S. Lebedev and V. I. Muromtsev, *EPR and Relaxation of Stabilized Radicals* (Khimija, Moscow, 1972).
- ⁴³P. R. Gullis, *J. Magn. Reson.* **21**, 397 (1976).
- ⁴⁴J. S. Hyde and L. R. Dalton, in *Spin Labeling. Theory and Application*, edited by L. Berliner (Academic Press, New York, 1979), Vol. 2, p. 1.
- ⁴⁵M. A. Butler, L. R. Walker, and Z. G. Soos, *J. Chem. Phys.* **64**, 3592 (1976).
- ⁴⁶A. Abragam, *The Principles of Nuclear Magnetism* (Clarendon Press, Oxford, 1961).
- ⁴⁷F. Devreux, F. Genoud, M. Nechtschein, and B. Villeret, in *Electronic Properties of Conjugated Polymers*, (Ref. 2), p. 270.
- ⁴⁸F. Zuo, M. Angelopoulos, A. G. MacDiarmid, and A. J. Epstein, *Phys. Rev. B* **39**, 3570 (1989).
- ⁴⁹F. Lux, Ph.D. thesis, Technology University of Berlin, 1993.
- ⁵⁰J. Patzsch and H. Gruber, in *Electronic Properties of Polymers*, (Ref. 2), p. 121.
- ⁵¹L. Zuppiroli, S. Paschen, and M. N. Bussac, *Synth. Met.* **69**, 621 (1995).
- ⁵²Y. Cao, S. Li, Z. Xue, and D. Guo, *Synth. Met.* **16**, 305 (1986).
- ⁵³E. P. Nakhmedov, V. N. Prigodin, and A. N. Samukhin, *Fiz. Tverd. Tela (Leningrad)* **31**, 64 (1989) [*Sov. Phys. Solid State* **31**, 368 (1989)].
- ⁵⁴F. J. Dyson, *Phys. Rev.* **98**, 349 (1955).
- ⁵⁵Z. Wilamowski, B. Oczkiewicz, P. Kacman, and J. Blinowski, *Phys. Status Solidi B* **134**, 303 (1986).

- ⁵⁶T. Sugano, G. Saito, and M. Kinoshita, *Phys. Rev. B* **35**, 6554 (1987).
- ⁵⁷P. Bernier, in *Handbook of Conducting Polymers*, edited by T. E. Scothorn (Marcel Dekker, Inc., New York, 1986), Vol. 2, p. 1099.
- ⁵⁸I. B. Goldberg, H. R. Crowe, P. R. Newman, A. J. Heeger, and A. G. MacDiarmid, *J. Chem. Phys.* **70**, 1132 (1979); R. L. Elsenbaumer, P. Delannoy, G. G. Muller, C. E. Forbes, N. S. Murthy, H. Eckhardt, and R. H. Baughman, *Synth. Met.* **11**, 251 (1985); R. Cosmo, E. Dormann, B. Gotschy, H. Naarmann, and H. Winter, *ibid.* **41**, 369 (1991); D. Billand, F. X. Henry, and Willmann, *ibid.* **69**, 9 (1995).
- ⁵⁹Y. W. Park, C. Park, Y. S. Lee, C. O. Yoon, H. Shirakawa, Y. Suezaki, and K. Akagi, *Solid State Commun.* **65**, 147 (1988); A. B. Kaiser, *Phys. Rev. B* **40**, 2806 (1989); J. Tsukamoto, A. Takahashi, and K. Kawasaki, *Jpn. J. Appl. Phys.* **29**, 125 (1989); Y. Nogami, H. Kaneko, T. Ishiguro, A. Takahashi, J. Tsukamoto, and N. Hosoi, *Solid State Commun.* **76**, 583 (1990); J. Tsukamoto and A. Takahashi, *Synth. Met.* **41-43**, 7 (1991).
- ⁶⁰L. Pietronero, *Synth. Met.* **8**, 225 (1983).
- ⁶¹K. Aasmundtveit, F. Genoud, E. Houzè, and M. Nechtschein, *Synth. Met.* **69**, 193 (1995).
- ⁶²T. N. Khazanovich, *Vysokomol. Soedin.* **5**, 112 (1963).
- ⁶³E. A. Silinsh, M. V. Kurik, and V. Chapek, *The Electronic Processes in Organic Molecular Crystals* (Zinatne, Riga, 1988).
- ⁶⁴The sensitivity of the ST-EPR method to the molecular dynamics decreases when the magnetic parameters of the PC are motionally averaged. As the correlation time of a macromolecular reorientations does not change considerably at the transition from sample I, to samples II, and III, we can propose the analogous character of chain librations in highly doped PANI samples the PC's of which are characterized by a motionally averaged magnetic parameters.
- ⁶⁵J. S. Blakemore, *Solid State Physics*, 2nd ed. (Cambridge University Press, Cambridge, 1985).